TASK QUARTERLY 14 No 3, 237–248

1D MODEL CALIBRATION BASED ON 3D CALCULATIONS FOR TESLA TURBINE

ROMUALD PUZYREWSKI AND KRZYSZTOF TESCH

Turbomachinery and Fluid Mechanics Department,
Gdansk University of Technology,
Narutowicza 11/12, 80-233 Gdansk, Poland
rpuzyrew@pg.gda.pl

(Received 14 June 2010; revised manuscript received 28 August 2010)

Abstract: This paper presents a system of equations for an axisymmetric laminar flow, after averaging, through the width of the interdisk slit of a Tesla turbine. Coefficients improving the efficiency of a 1D model were introduced as a result of averaging. The minimal number of such coefficients was determined. The 1D model makes it possible to attain analytical solutions to an accuracy limited by these coefficients. The calibration of a 1D model depends on finding the numerical values of coefficients that yield a sufficient accuracy compared with 3D calculations. A definition of the efficiency coefficient for the Tesla turbine is also given. This definition relies on the 1D model results. Example values of this coefficient are described after the 1D model calibration.

Keywords: turbomachinery, Tesla turbine, 1D model

1. Introduction

The literature on Tesla's patent [1] concerning bladeless conversion of fluid energy is relatively wide [2]. It is related to both pumps and turbines. The attractiveness of such a design relies on its simplicity. This is due to the lack of blades. From a practical point of view, the lack of a widespread use of such turbines can be explained by the low efficiency. This design takes advantage only of a friction mechanism for energy conversion and eliminates a mechanism of the lift force which is characteristic for blade machines. Much attention was paid to the Tesla turbine from the viewpoint of fluid mechanics. It seemed that the structural simplicity of this solution could allow a simple solution of the basic equations of fluid mechanics, *i.e.* the Navier-Stokes (N-S) equations. As it turned out, the conversion of partial differential equations (N-S) to ordinary differential equations, by changing the variables which would allow obtaining the so called self-similar solution [3], was not possible. Such attempts were undertaken in the 70s of the last century. Recently, numerical solutions have been used. From the

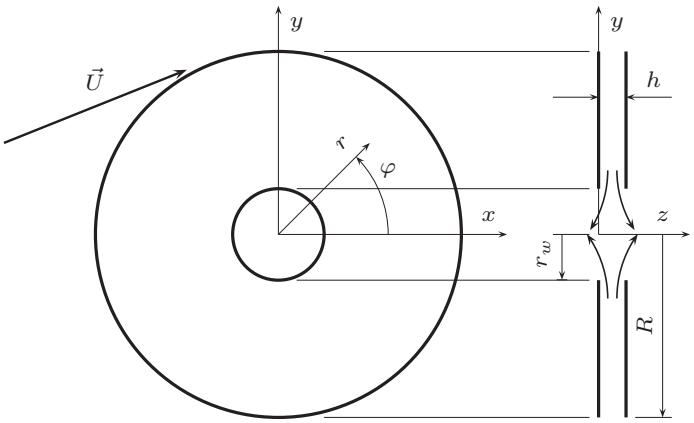

Figure 1. Tesla turbine flow system

technical point of view they are sufficient to evaluate the change of the parameters in a Tesla turbine flow system (shown in Figure 1).

Analytical solutions of the equation system for the interdisk slit are possible for the 1D model after averaging through the slit height, h. A comparison of the 1D and 3D calculations for a stage of Tesla turbine makes it possible to fit coefficients arriving in the 1D model. A variant of the 1D model that differs from that of Rice [4] was proposed. The differences are due to the derivation of an equation system of the model as well as frictional force modelling. The coordinate system was adopted as in Figure 1. The power supply of the slit h between the discs is carried out on the outer radius of R by means of the jet with speed U having a circumferential and radial component.

2. Simplification of N-S equation

Let us introduce some simplifications to a closed system of N-S equations rewritten in cylindrical coordinates. Radial velocity components, tangential and axial are indicated by U_r, U_φ, U_z, respectively.

The system contains the mass conservation equation and three equations of motion, and is closed. The unknown functions are: velocity components U_r, U_φ, U_z and pressure p. Assuming $\rho = \text{const.}$, $\frac{\partial}{\partial t}$, $\frac{\partial}{\partial \varphi}$ the system of equations is [5]:

$$\frac{\partial U_r}{\partial r} + \frac{U_r}{r} + \frac{\partial U_z}{\partial z} = 0 \tag{1a}$$

$$\rho\left(U_r\frac{\partial U_r}{\partial r} - \frac{U_\varphi^2}{r} + U_z\frac{\partial U_r}{\partial z}\right) = -\frac{\partial p}{\partial r} + \mu\left(\frac{\partial^2 U_r}{\partial r^2} + \frac{1}{r}\frac{\partial U_r}{\partial r} - \frac{U_r}{r^2} + \frac{\partial^2 U_r}{\partial z^2}\right) \tag{1b}$$

$$\rho\left(U_r\frac{\partial U_\varphi}{\partial r} + \frac{U_\varphi U_r}{r} + U_z\frac{\partial U_\varphi}{\partial z}\right) = \mu\left(\frac{\partial^2 U_\varphi}{\partial r^2} + \frac{1}{r}\frac{\partial U_\varphi}{\partial r} - \frac{U_\varphi}{r^2} + \frac{\partial^2 U_\varphi}{\partial z^2}\right) \tag{1c}$$

$$\rho\left(U_r\frac{\partial U_z}{\partial r} + U_z\frac{\partial U_z}{\partial z}\right) = -\frac{\partial p}{\partial z} + \mu\left(\frac{\partial^2 U_z}{\partial r^2} + \frac{1}{r}\frac{\partial U_z}{\partial r} + \frac{\partial^2 U_z}{\partial z^2}\right) \tag{1d}$$

Let us introduce the dimensionless parameters on the basis of two linear scales $h \ll R$ and two velocity scales $W \ll U$ in the following form $r = R\bar{r}$, $z = h\bar{z}$, $U_r = U\bar{U}_r$, $U_\varphi = U\bar{U}_\varphi$, $U_z = W\bar{U}_z$, $p = \rho U^2 \bar{p}$. Neglecting the overbars and assuming the following estimates $h = \epsilon_r R$, $\epsilon_r \ll 1$, $W = \epsilon_u U$, $\epsilon_u \ll 1$ the system of equations takes the form:

$$\frac{\partial U_r}{\partial r} + \frac{U_r}{r} + \frac{\epsilon_u}{\epsilon_r}\frac{\partial U_z}{\partial z} = 0 \tag{2a}$$

$$U_r\frac{\partial U_r}{\partial r} - \frac{U_\varphi^2}{r} + \frac{\epsilon_u}{\epsilon_r}U_z\frac{\partial U_r}{\partial z} = -\frac{\partial p}{\partial r} + \frac{1}{Re}\left(\frac{\partial^2 U_r}{\partial r^2} + \frac{1}{r}\frac{\partial U_r}{\partial r} - \frac{U_r}{r^2}\right) + \frac{1}{\epsilon_r^2 Re}\left(\frac{\partial^2 U_r}{\partial z^2}\right) \tag{2b}$$

$$U_r\frac{\partial U_\varphi}{\partial r} + \frac{U_\varphi U_r}{r} + \frac{\epsilon_u}{\epsilon_r}U_z\frac{\partial U_\varphi}{\partial z} = \frac{1}{Re}\left(\frac{\partial^2 U_\varphi}{\partial r^2} + \frac{1}{r}\frac{\partial U_\varphi}{\partial r} - \frac{U_\varphi}{r^2}\right) + \frac{1}{\epsilon_r^2 Re}\left(\frac{\partial^2 U_\varphi}{\partial z^2}\right) \tag{2c}$$

$$U_r\frac{\partial U_z}{\partial r} + \frac{\epsilon_u}{\epsilon_r}U_z\frac{\partial U_z}{\partial z} = -\frac{1}{\epsilon_u\epsilon_r}\frac{\partial p}{\partial z} + \frac{1}{Re}\left(\frac{\partial^2 U_z}{\partial r^2} + \frac{1}{r}\frac{\partial U_z}{\partial r}\right) + \frac{1}{\epsilon_r^2 Re}\frac{\partial^2 U_z}{\partial z^2} \tag{2d}$$

The Reynolds number is defined here as $\mathrm{Re} = \rho U R \mu^{-1}$.

3. Averaging through the z coordinate

Assuming that $\epsilon_u \approx \epsilon_r$ allows us to simplify the system:

$$\frac{1}{r}\frac{\partial}{\partial r}(rU_r) + \frac{\partial U_z}{\partial z} = 0 \tag{3a}$$

$$\rho\left(U_r\frac{\partial U_r}{\partial r} - \frac{U_\varphi^2}{r} + U_z\frac{\partial U_r}{\partial z}\right) = -\frac{\mathrm{dp}}{\mathrm{dr}} + \frac{\partial \tau_r}{\partial z} \tag{3b}$$

$$\rho\left(U_r\frac{\partial U_\varphi}{\partial r} + \frac{U_\varphi U_r}{r} + U_z\frac{\partial U_\varphi}{\partial z}\right) = \frac{\partial \tau_\varphi}{\partial z} \tag{3c}$$

$$\frac{\partial p}{\partial z} \approx 0 \tag{3d}$$

Pressure p depends only on the r coordinate. This is true, however, within the accuracy of terms ϵ^2. Instead of second derivatives we use the first derivative of tangential stresses $\tau_r = \mu\frac{\partial U_r}{\partial z}$, $\tau_\varphi = \mu\frac{\partial U_\varphi}{\partial z}$. The mass conservation equation is averaged through z from 0 to h:

$$\frac{1}{r}\frac{\partial}{\partial r}\left(\frac{r}{h}\int_0^h U_r\,\mathrm{d}z\right) + \frac{1}{h}\int_0^h \frac{\partial U_z}{\partial z}\,\mathrm{d}z = 0 \tag{4}$$

Using the condition $U_z = 0$ for $z = 0$ and $z = h$ we obtain the average component of velocity $\tilde{U}_r = \frac{1}{h}\int_0^h U_r\,\mathrm{d}z$ which is now a function only of component r:

$$\tilde{U}_r = -\frac{1}{r}U_q R = -\frac{Q}{2\pi r h} \tag{5}$$

where Q represents the volumetric flow rate and is prescribed by means of the radial velocity component at inlet U_q.

The averaged U_z component disappears in conservation equations. This is due to the asymmetry of U_z:

$$\frac{1}{h}\int_0^h U_z\frac{\partial U_r}{\partial z}\,\mathrm{d}z=\frac{1}{h}\frac{\widetilde{\partial U_r}}{\partial z}\int_0^h U_z\,\mathrm{d}z=0 \tag{6a}$$

$$\frac{1}{h}\int_0^h U_z\frac{\partial U_\varphi}{\partial z}\,\mathrm{d}z=\frac{1}{h}\frac{\widetilde{\partial U_\varphi}}{\partial z}\int_0^h U_z\,\mathrm{d}z=0 \tag{6b}$$

Introducing the average $\tilde{U}_\varphi=\frac{1}{h}\int_0^h U_\varphi\,\mathrm{d}z$ allows us to write:

$$\frac{1}{h}\int_0^h U_r\frac{\partial U_r}{\partial r}\,\mathrm{d}z=\frac{1}{2h}\frac{\partial}{\partial r}\int_0^h U_r^2\,\mathrm{d}z=\frac{1}{2}\frac{\mathrm{d}\widetilde{\mathrm{U}_\mathrm{r}^2}}{\mathrm{dr}}=C_{rr}\frac{1}{2}\frac{\mathrm{d}\tilde{\mathrm{U}}_\mathrm{r}^2}{\mathrm{dr}}=C_{rr}\tilde{U}_r\frac{\mathrm{d}\tilde{\mathrm{U}}_\mathrm{r}}{\mathrm{dr}} \tag{7a}$$

$$\frac{1}{h}\int_0^h U_r\frac{\partial U_\varphi}{\partial r}\,\mathrm{d}z=\frac{\hat{U}_r}{h}\frac{\partial}{\partial r}\int_0^h U_\varphi\,\mathrm{d}z=C_{r\varphi}\tilde{U}_r\frac{\mathrm{d}\tilde{\mathrm{U}}_\varphi}{\mathrm{dr}} \tag{7b}$$

$$\frac{1}{h}\int_0^h\frac{U_\varphi^2}{r}\,\mathrm{d}z=\frac{1}{hr}\int_0^h U_\varphi^2\,\mathrm{d}z=\frac{\widetilde{U_\varphi^2}}{r}=C_{\varphi\varphi}\frac{\tilde{U}_\varphi^2}{r} \tag{7c}$$

$$\frac{1}{h}\int_0^h\frac{U_\varphi U_r}{r}\,\mathrm{d}z=\frac{\hat{\tilde{U}}_r}{hr}\int_0^h U_\varphi\,\mathrm{d}z=C_{\varphi r}\frac{\tilde{U}_\varphi\tilde{U}_r}{r} \tag{7d}$$

In the above relations the coefficients, C_{rr}, $C_{\varphi\varphi}$, $C_{r\varphi}$, $C_{\varphi r}$ are introduced. They are also called Coriolis coefficients and they allow us to improve the following estimates:

$$\widetilde{U_r^2}\approx\tilde{U}_r^2,\widetilde{U_\varphi^2}\approx\tilde{U}_\varphi^2,\hat{U}_r\approx\tilde{U}_r,\hat{\tilde{U}}_r\approx\tilde{U}_r \tag{8}$$

Without simplifications it is possible to introduce averaged wall stresses:

$$\frac{1}{h}\int_0^h\frac{\partial\tau_r}{\partial z}\,\mathrm{d}z=\frac{\tau_r(z)|_0^h}{h}=\frac{2\tau_r}{h} \tag{9}$$

$$\frac{1}{h}\int_0^h\frac{\partial\tau_\varphi}{\partial z}\,\mathrm{d}z=\frac{\tau_\varphi(z)|_0^h}{h}=\frac{2\tau_\varphi}{h} \tag{10}$$

The system of equations for the 1D model can now be written as:

$$\rho\left(C_{rr}\tilde{U}_r\frac{\mathrm{d}\tilde{\mathrm{U}}_\mathrm{r}}{\mathrm{dr}}-C_{\varphi\varphi}\frac{\tilde{U}_\varphi^2}{r}\right)=-\frac{\mathrm{dp}}{\mathrm{dr}}+\frac{2\tau_r}{h} \tag{11a}$$

$$\rho\left(C_{r\varphi}\tilde{U}_r\frac{\mathrm{d}\tilde{\mathrm{U}}_\varphi}{\mathrm{dr}}-C_{\varphi r}\frac{\tilde{U}_\varphi\tilde{U}_r}{r}\right)=-\frac{2\tau_\varphi}{h} \tag{11b}$$

The signs of stresses τ_r oraz τ_φ are included in the above system, see Figure 2. This is not true for the velocity component. As can be seen in Figure 2 we have $U_r<0$ and $U_\varphi>0$. The velocity vector fields of velocity components in the transverse cross section of the disc slit are shown in Figure 3.

To estimate stress τ components we take advantage of the following proportions $\tau_r\sim\tilde{U}_rh^{-1}$, $\tau_\varphi\sim(\tilde{U}_\varphi-\omega r)h^{-1}$. Introducing the velocity profile coefficients k_r and k_φ the stress components can be written as $\tau_r=\mu\frac{\partial U_r}{\partial z}|_{z=0,h}=\mu k_rh^{-1}\tilde{U}_r(r)$, $\tau_\varphi=\mu\frac{\partial}{\partial z}(U_\varphi-\omega r)|_{z=0,h}=\mu k_\varphi h^{-1}(\tilde{U}_\varphi-\omega r)=\mu k_\varphi h^{-1}U_s(r)$. For

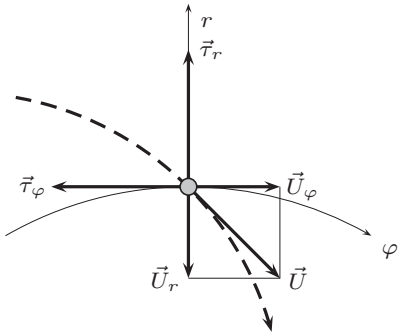

Figure 2. Stress components and velocities

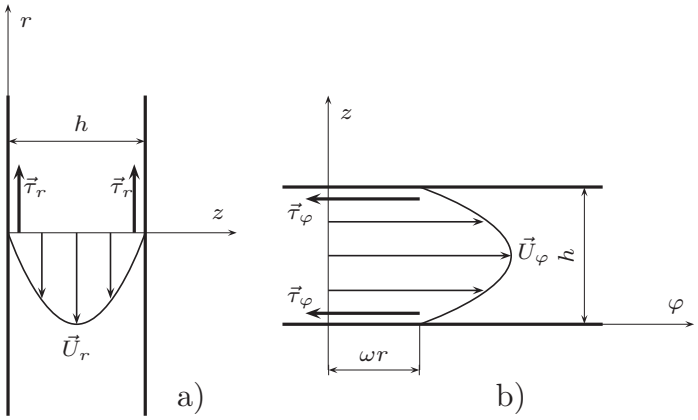

Figure 3. Velocity field in transverse cross section

the circumferential velocity component we have $U_\varphi = \omega r + U_s(r)$ as can be seen in Figure 3b. It can be easily checked that for the parabolic velocity profile the velocity profile coefficient $k_{r,\varphi} = 6$. This is true for laminar flows in straight channels.

In the equation system (11) we have 6 coefficients. Four of them are of the C- and two of the k-type. It is impossible to calculate these coefficients without knowing the velocity profiles *a priori*. The equations of motions limit the number of coefficients in Equation (11b). Multiplying this equation by $2\pi r^2 h$ we have $2\pi r h \rho \tilde{U}_r (C_{r\varphi} r \,\mathrm{d}\tilde{U}_\varphi + C_{\varphi r} \tilde{U}_\varphi) = -4\pi r^2 \tau_\varphi \,\mathrm{d}r$. This further leads to a momentum conservation equation under the condition that $C_{\varphi r} = C_{r\varphi} = C$. Then:

$$mC \int_{r_w}^{R} \mathrm{d}\left(r\tilde{U}_\varphi\right) = 4\pi \int_{r_w}^{R} r^2 \tau_\varphi \,\mathrm{d}r \tag{12}$$

where $m = \rho Q$ stands for the mass flow rate. Assuming that k_φ is constant, the integral form of the angular momentum conservation equation is:

$$m\left(\left(R\tilde{U}_\varphi\right)_0 - \left(r_w \tilde{U}_\varphi\right)_w\right) = \frac{4K_\varphi \pi \mu}{h} \int_{r_w}^{R} r^2 U_s(r) \,\mathrm{d}r \tag{13}$$

where $K_\varphi = k_\varphi C^{-1}$. The change of the angular momentum between inlet (subscript 0) and outlet (subsript w) equals the momentum captured by means of shear stresses on discs. This condition allows us to reduce the number of coefficients in the momentum conservation equation towards φ direction. We have now one coefficient K_φ.

Equation (11b) in the following form:

$$\rho\left(\frac{RU_q}{r}\left(\omega+\frac{\mathrm{dU_s(r)}}{\mathrm{dr}}\right)\right)+\frac{RU_q(\omega r+U_s(r))}{r^2}=\frac{2K_\varphi\mu U_s(r)}{h^2} \tag{14}$$

is integrable and gives an analytical solution for $U_s(r)$:

$$\tilde{U}_\varphi=\omega r+\frac{R}{r}U_{s0}\exp\frac{\mu K_\varphi(r^2-R^2)}{\rho h^2 RU_q}+\frac{R\rho\omega h^2U_q}{r\mu K_\varphi}\left(1-\exp\frac{\mu K_\varphi(r^2-R^2)}{\rho h^2 RU_q}\right) \tag{15}$$

with an initial condition $U_s(R)=U_{s0}$. We have two special cases here for $\tilde{U}_\varphi$. If $\mu K_\varphi\to 0$, which corresponds to an inviscid flow, then $\tilde{U}_\varphi\to(U_{s0}+\omega R)Rr^{-1}$. The second case is when $\mu K_\varphi\to\infty$ which corresponds to a creeping flow. Then, we have $\tilde{U}_\varphi\to\omega r$ which describes a motion analogical to the motion of a solid.

Equation (11a) contains three coefficients C_{rr}, $C_{\varphi\varphi}$, k_r. Further reduction is possible $C_{rr}=C_{\varphi\varphi}=C_r$ but it reduces the degree of freedom in terms of matching 1D and 3D results. We can rewrite Equation (11a):

$$C_r\rho\left(\tilde{U}_r\frac{\mathrm{d\tilde{U}_r}}{\mathrm{dr}}-\frac{\tilde{U}_\varphi^2}{r}\right)=-\frac{\mathrm{dp}}{\mathrm{dr}}+\frac{2\mu k_r\tilde{U}_r}{h^2} \tag{16}$$

This equation allows integrating p analytically together with the boundary condition, $p=p_0$. Without prejudice to generality it can be assumed that $p_0=0$.

It is possible to introduce τ_r and τ_φ for the average trajectory. This is true under the condition that the directions of τ_r oraz τ_φ are taken into consideration:

$$\tau_r=\tau\frac{\left|\tilde{U}_r\right|}{U}=\tau\frac{\left|\tilde{U}_r\right|}{\sqrt{\tilde{U}_r^2+\tilde{U}_\varphi^2}},\quad \tau_\varphi=\tau\frac{\tilde{U}_\varphi}{U}=\tau\frac{\tilde{U}_\varphi}{\sqrt{\tilde{U}_r^2+\tilde{U}_\varphi^2}} \tag{17}$$

The location of stresses inside the channel is shown in Figure 3 with respect to the coordinate system r and φ. Further we have:

$$\rho\left(C_{rr}\tilde{U}_r\frac{\mathrm{d\tilde{U}_r}}{\mathrm{dr}}-C_{\varphi\varphi}\frac{\tilde{U}_\varphi^2}{r}\right)=-\frac{\mathrm{dp}}{\mathrm{dr}}+\frac{2\tau\left|\tilde{U}_r\right|}{h\sqrt{\tilde{U}_r^2+\tilde{U}_\varphi^2}} \tag{18a}$$

$$\rho\left(C_{r\varphi}\tilde{U}_r\frac{\mathrm{d\tilde{U}_\varphi}}{\mathrm{dr}}-C_{\varphi r}\frac{\tilde{U}_\varphi\tilde{U}_r}{r}\right)=-\frac{2\tau\tilde{U}_\varphi}{h\sqrt{\tilde{U}_r^2+\tilde{U}_\varphi^2}} \tag{18b}$$

Eliminating $\tilde{U}_\varphi=\sqrt{U^2-\tilde{U}_r^2}$ from the above system one can see that:

$$\frac{\mathrm{dp}}{\mathrm{dr}}=\frac{\rho\tilde{U}_r^2}{r}+\frac{2\tau\left|\tilde{U}_r\right|}{hU} \tag{19a}$$

$$\frac{\mathrm{d}}{\mathrm{d}r}\ln(Ur) = -\frac{2\tau}{\rho h U \tilde{U}_r}\left(1-\frac{\tilde{U}_r^2}{U^2}\right) \tag{19b}$$

Alternatively, the second equation can be also written as:

$$\frac{\mathrm{dU}}{\mathrm{d}r}+\frac{U}{r} = -\frac{2\tau}{\rho h \tilde{U}_r}\left(1-\frac{\tilde{U}_r^2}{U^2}\right) \tag{19b$'$}$$

The shear stress $\tau = \sqrt{\tau_r^2+\tau_\varphi^2}$ may be expressed as:

$$\tau = \frac{\mu}{h}\sqrt{k_r^2\tilde{U}_r^2+k_\varphi^2(\tilde{U}_\varphi-\omega r)^2} \tag{20}$$

4. 3D calculations

Example 3D calculations were performed within a stage of the Tesla turbine. The geometry of a disk was taken into consideration. The outlet radius $R = 0.06\,\mathrm{m}$, inlet radius $r_w = 0.0075\,\mathrm{m}$, disk slit height $h = 0.001\,\mathrm{m}$, angular velocity $\omega = 10\,\mathrm{s}^{-1}$. The density of water $\rho = 1000\,\mathrm{kg\,m}^{-3}$ and molecular velocity $\mu = 0.001\,\mathrm{kg\,m}^{-1}\mathrm{s}^{-1}$.

It was only $\frac{1}{10}^{\mathrm{th}}$ of the original geometry that was considered. This is due to the periodicity of the geometry and the boundary condition. The steady state equation system (N-S) was solved by means of the Finite Volumes Method by commercial code CFX. The flow was laminar because of a small Reynolds number (Re = 500 at the inlet).

4.1. Boundary conditions

The boundary conditions were the following:

- Inlet: The velocity components in steady state coordinates were: $U_z = 0$, $U_r = -0.5\,\mathrm{ms}^{-1}$, $U_\varphi = 1\,\mathrm{ms}^{-1}$ ($U_s = 0.4\,\mathrm{ms}^{-1}$).
- Outlet: Constant pressure distribution was prescribed in rotating coordinates. The pressure was set equal to the atmospheric pressure.
- Periodicity: The surfaces which were created by sectoring of the full cylinder were identified as periodic surfaces. Periodicity is understood here as rotation of 36°.
- Walls: The upper and lower surfaces (disks) were treated as impenetrable, non-slip walls in rotating coordinates.

4.2. Discretisation

The geometry was discretised by means of tetrahedral and prismatic elements. The mesh was unstructured and composed of ∼0.7 million elements. Prismatic elements are placed near the wall where high velocity gradients are expected, see Figure 4. Mesh statistics are presented in Table 1.

Table 1. Mesh statistics

Element type	Number
Tetrahedral	281540
Prismatic	420900
Total	702440

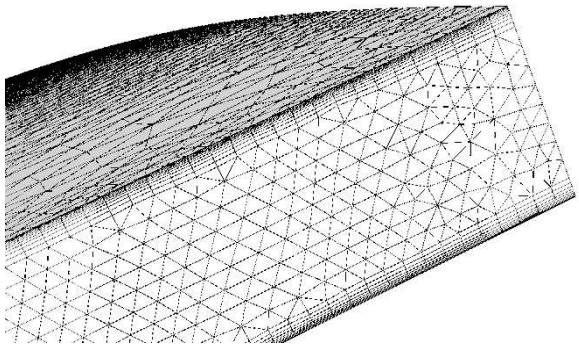

Figure 4. Mesh

Figure 5 presents the velocity component U_r distribution along the slit height for different radii. The average value of this component increases due to a decrease in the cross section according to Equation (5). Characteristic local maximal values may be observed near the walls starting from $r \approx 0.02\,\mathrm{m}$. They come about because the mass flow rate is shifted from the channel centre towards the walls. This is confirmed by a pressure difference in the transverse cross-section which is higher in the channel centre and lower near the walls.

The axial velocity follows this tendency of pressure difference, see Figure 6. The visible asymmetry of U_z distribution is due to mass transport from the channel centre towards the walls. This explains local maximal values of U_r. The asymmetry of U_z also justifies the results of averaging of Equations (6).

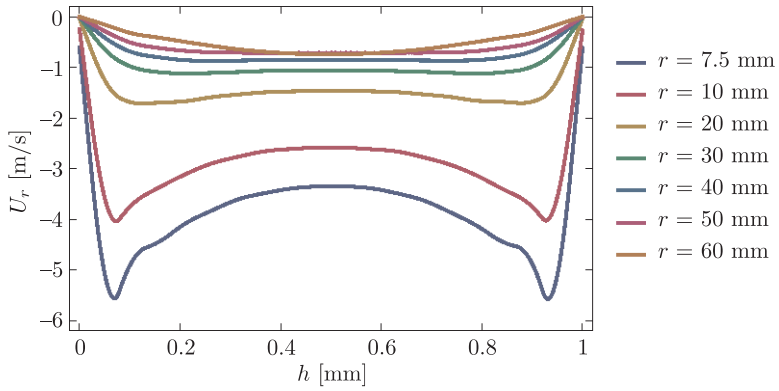

Figure 5. U_r distribution

5. 1D model calibration

By calibration of a 1D model by a 3D model we mean such a choice of coefficients C_r, k_r, K_φ which allows for an accuracy good enough to match between these two models. We consider here the velocity components and pressure difference Δp as a function of radius. By good enough accuracy one understands the accuracy in the sense of engineering intuition such as it is shown in figures

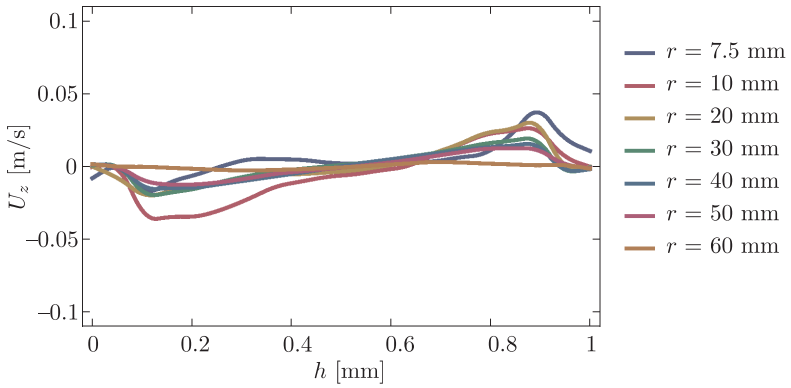

Figure 6. U_z distribution

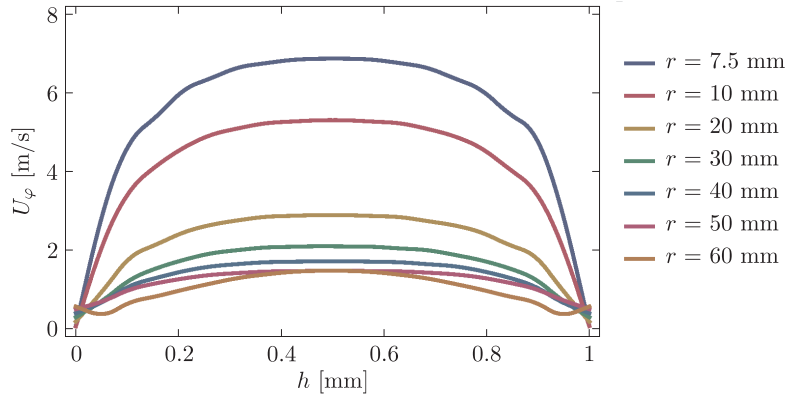

Figure 7. U_φ distribution

showing a comparison of results between 1D and 3D models. The radial component U_r comes in both the 1D and 3D models from the mass conservation equation. This gives very good agreement of the average value of this component.

Figures 8 and 9 show a comparison of the averaged U_φ component and pressure difference Δp. The assumed values of the 1D model coefficients were: $k_r = 6.0$, $k_\varphi = 4.476402$, $C_{r\varphi} = C_{\varphi r} = 1.0$, $K_\varphi = 4.476402$, $C_r = C_{rr} = C_{\varphi\varphi} = 1.165$. It should be borne in mind that the pressure difference cannot exceed certain values related to the phenomenon of cavitation. For the 3D calculation the parabolic velocity profile was prescribed on the outer radius.

6. Efficiency

In order to define the efficiency of power collection from the flow we need to bring the system of Equations (11) to the form of energy equation. To do this we multiply Equation (11a) by U_r and Equation (11b) by U_φ. After summation we have:

$$\rho U_r \frac{\mathrm{d}}{\mathrm{d}r}\left(\frac{U^2}{2} + \frac{p}{\rho}\right) = \frac{2}{h}\left(\tau_r U_r - \tau_\varphi U_\varphi\right) < 0 \tag{21}$$

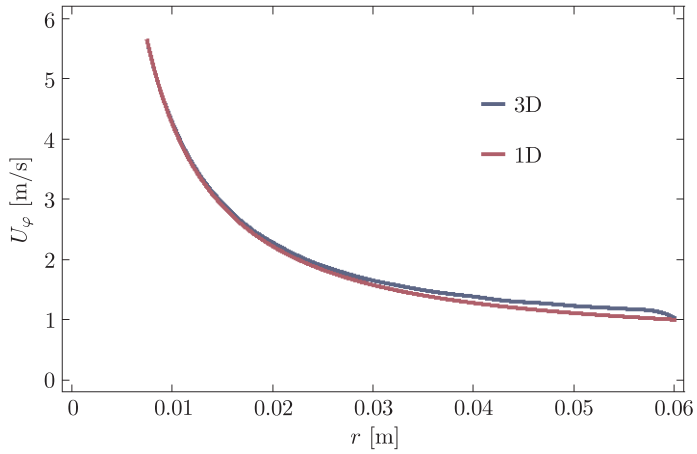

Figure 8. U_φ distribution

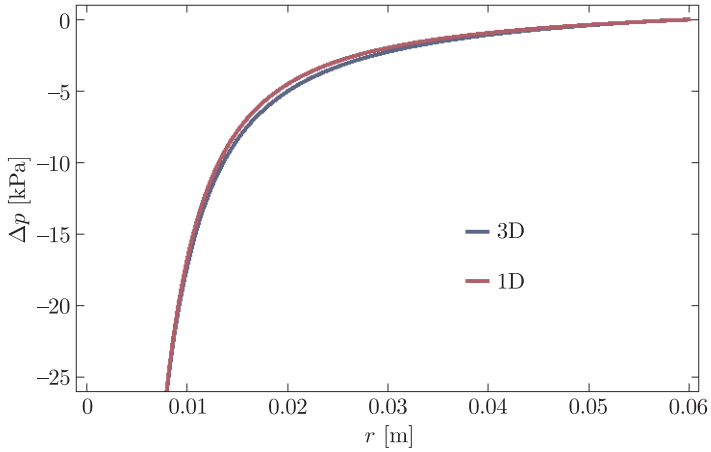

Figure 9. Δp distribution

It can be seen that for $U_r < 0,\ \mathrm{d}r < 0$ and negative left hand side of the above equation we have a decrease in total energy. For the effect of power extraction (turbine effect) we must have:

$$\mathrm{d}\left(\frac{U^2}{2}+\frac{p}{\rho}\right) < 0 \tag{22}$$

By means of mass conservation equation $2\pi r h \rho U_r = \text{const.}$ it is possible to find the power difference between inlet radius R and outlet radius r_w:

$$\begin{aligned}\Delta N &= 2\pi R h \rho |U_r| \left(\frac{U^2}{2}+\frac{p}{\rho}\right)\Big|_R - 2\pi r_w h \rho |U_r| \left(\frac{U^2}{2}+\frac{p}{\rho}\right)\Big|_{r_w} = \\ &= -4\pi \int_{r_w}^{R} r\,(\tau_r U_r - \tau_\varphi U_\varphi)\,\mathrm{d}r > 0\end{aligned} \tag{23}$$

This difference is due to viscosity which is responsible for wall stress generation on disk walls. It is only a portion of this power difference that is used in an effective form (extracted by disks). This part can be expressed by an angular momentum for two disk surfaces:

$$M = 2\int_0^{2\pi}\int_{r_w}^{R} r^2 \tau_\varphi \,\mathrm{d}\varphi\,\mathrm{d}r \tag{24}$$

which gives the effective power

$$\Delta N_e = M\omega = \frac{4\pi\mu k_\varphi \omega}{h}\int_{r_w}^{R} r^2\left(\sqrt{U^2 - U_r^2} - \omega r\right)\mathrm{d}r \tag{25}$$

The rest of the power due to the total energy difference is the dissipation power ΔN_d because of viscosity $\Delta N_d = \Delta N - \Delta N_e$. Efficiency can now be defined as the following ratio:

$$\eta_e = \frac{\Delta N_e}{\Delta N} \tag{26}$$

It should be stressed that the referential power is not the power of an ideal (inviscid) process as it is in blade turbines. This is simply because for an ideal process one cannon obtain power from Tesla turbine. The distribution of efficiency for three different disk slit thickness values is shown in Figure 10. The flatness of this distribution as a function of ω is visible. However, the level of the horizontal asymptote depends strongly on disk slit thickness, h.

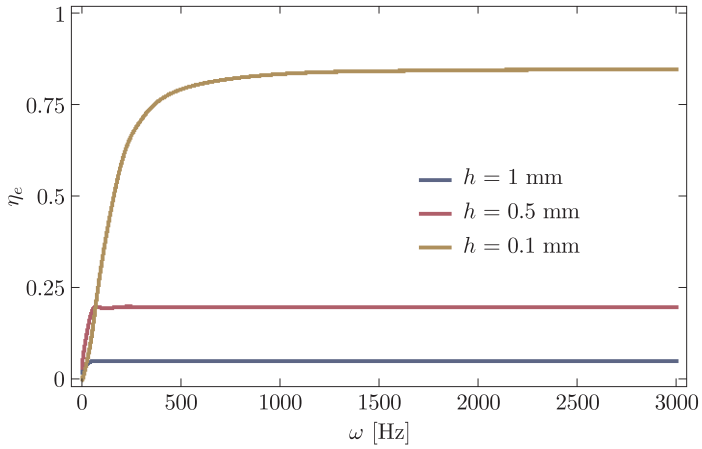

Figure 10. Efficiency

The influence of angular velocity ω on the maximal value is small. It can only by observed on further significant decimal places. Within the range of the graph in Figure 10 maximal values are not visible.

7. Conclusions

- It is possible to calibrate the 1D model on the basis of 3D calculations. When the 1D model is calibrated it allows calculating the efficiency of energy extraction from the flow to disks in a very simple way.

- Efficiency strongly depends on the disk slit thickness. Relatively high values of efficiency can be obtained for a very low thickness. Unfortunately, this leads to low power of a stage which is proportional to the mass flow rate.

References

[1] Tesla N 1913 *Turbine*, *U.S. Patent No. 1061206*
[2] Rey Ladino A F 2004 *Numerical Simulation of the Flow Field in Friction-Type Turbine (Tesla Turbine)*, *Diploma Thesis at Technische Universität Wien*, Vienna
[3] McAlister K W and Rice W 1970 *J. Appl. Mech.* **37** (4) 924
[4] Rice W 1965 *J. Eng. for Power* **87** (1) 29
[5] Puzyrewski R 1992 *Fundamentals of Turbomachinery Theory - One Dimensional Approach*, Ossolineum, Wroclaw, Poland (in Polish)